Simulation of domain formation in DLPC-DSPC mixed bilayers

ARTICLE *in* LANGMUIR · SEPTEMBER 2004

Impact Factor: 4.46 · DOI: 10.1021/la0492759 · Source: PubMed

2 AUTHORS:

Roland Faller
University of California, Davis
161 PUBLICATIONS **2,654** CITATIONS
SEE PROFILE

Siewert J Marrink
University of Groningen
216 PUBLICATIONS **14,144** CITATIONS
SEE PROFILE

Simulation of Domain Formation in DLPC−DSPC Mixed Bilayers

Roland Faller*

Department of Chemical Engineering & Materials Science, University of California−Davis, Davis, California 95616

Siewert-Jan Marrink

Department of Biophysical Chemistry, University of Groningen, Groningen, The Netherlands

Received March 19, 2004. In Final Form: June 17, 2004

Binary mixtures of two phosphatidylcholines of different chain lengths are simulated in the bilayer state. We find a phase transition between a liquid state and a gel state at all concentrations. This phase transition is characterized by the area per lipid headgroup, the order parameter, and a change in dynamics. At concentrations with a majority of the longer lipid, we find phase separation into a gel and a liquid state in a small temperature window. This leads to a strong dynamic heterogeneity. Experimental phase transition temperatures are reproduced semiquantitatively. We see a clear shift in the phase transition to higher temperatures with increasing concentration of the longer lipid.

1. Introduction

Phospholipid bilayers play an important role in the circle of life as they constitute cellular and intracellular membranes. So it is not surprising that there is a wealth of research devoted to them. Computer simulations play an increasing role in this field. But although it is well-known that biologically relevant lipid bilayers contain more than one lipid in addition to a number of other molecules, computer simulations to date have mainly focused on bilayers of pure lipids[1] and lipid/cholesterol mixtures (e.g., ref 2).

Only recently, a number of studies on binary phospholipid systems have appeared,[3−6] using full atomistic detail. Nonideal mixing behavior of the components is not observed, however. To study domain formation or phase separation, much longer time scales should be addressed than is possible with atomistic simulations (currently limited to the nanosecond time scale). Using very simplified force fields, on the other hand, it is possible to predict the phase diagram of phospholipid-like molecules (e.g., ref 7).

Monte Carlo simulations using two-[8] or multistate[9] lattice models of DMPC−DSPC (dimyristoylphosphatidylcholine−distearoylphosphatidylcholine) mixtures show domain formation within a certain range of compositions. Domain sizes in qualitative agreement with experimental observations are predicted,[8] and domain growth is shown to be governed by nonequilibrium dynamics.[9] More quantitative predictions can be obtained by an intermediate approach, in which atomistic simulations are used as input to deduce coarse-grained parameters. A number of such coarse-grained models have been proposed.[10−12]

Coarse-graining (CG) is to date the only viable approach to reach into the relevant time and length scales for complex fluids such as polymers[13] and biomembranes.[10−12] However, any coarse-graining approach has to balance specificity toward the problem of study against computer speed. All-atom simulations of complex systems allow direct access to any interesting property for a specific system but are limited to time scales of a few nanoseconds. Very simplified generic approaches such as bead spring models[7,14] alleviate the problem of the short time scale but at the cost of loss of specificity. With such models, differences between individual models cannot be discerned. Therefore models mapping 5−8 heavy atoms into one interaction center have been proven to be a good compromise.[15] On this degree of detail, we can keep some specific information about the molecules while giving up a quantitative in favor of a semiquantitative description which still can distinguish between subclasses of molecules.

Another incentive for using coarse-grained models is the easier handling of the computationally costly electrostatics. In coarse-grained modeling, the effective in-

* To whom correspondence should be addressed. E-mail: rfaller@ucdavis.edu.

(1) Tieleman, D. P.; Marrink, S. J.; Berendsen, H. J. C. *Biochim. Biophys. Acta* (*Rev. Biomem.*) **1997**, *1331*, 235−270.
(2) Hofsass, C.; Lindahl, E.; Edholm, O. *Biophys. J.* **2003**, *84*, 2192−2206.
(3) Roy, D.; Mukhopadhyay, C. *J. Biomol. Struct. Dyn.* **2002**, *19*, 1121−1132.
(4) Pandit, S. A.; Bostick, D.; Berkowitz, M. L. *Biophys. J.* **2003**, *85*, 3120−3131.
(5) Balali-Mood, K.; Harroun, T. A.; Bradshaw, J. P. *Eur. Phys. J. E* **2003**, *12*, S135−S140.
(6) de Vries, A. H.; Mark, A. E.; Marrink, S. J. *J. Phys. Chem. B* **2004**, *108*, 2454−2463.
(7) Kranenburg, M.; Venturoli, M.; Smit, B. *J. Phys. Chem. B* **2003**, *107*, 11491−11501.
(8) Michonova-Alexova, E. I.; Sugar, I. P. *Biophys. J.* **2002**, *83*, 1820−1833.
(9) Jorgensen, K.; Klinger, A.; Biltonen, R. L. *J. Phys. Chem. B* **2000**, *104*, 11763−11773.
(10) Shelley, J. C.; Shelley, M. Y.; Reeder, R. C.; Bandyopadhyay, S.; Klein, M. L. *J. Phys. Chem. B* **2001**, *105*, 4464−4470.
(11) Ayton, G.; Voth, G. A. *Biophys. J.* **2002**, *83*, 3357−3370.
(12) Marrink, S. J.; de Vries, A.; Mark, A. *J. Phys. Chem. B* **2004**, *108*, 750−760.
(13) Baschnagel, J.; Binder, K.; Doruker, P.; Gusev, A. A.; Hahn, O.; Kremer, K.; Mattice, W. L.; Müller-Plathe, F.; Murat, M.; Paul, W.; Santos, S.; Suter, U. W.; Tries, V. *Adv. Polym. Sci.* **2000**, *152*, 41−156.
(14) Müller, M.; Katsov, K.; Schick, M. *J. Polym. Sci., Part B: Polym. Phys.* **2003**, *41*, 1441−1451.
(15) Faller, R. *Polymer* **2004**, *45*, 3869−3876.

10.1021/la0492759 CCC: $27.50
Published on Web 07/31/2004

teraction between the charges can be successfully reproduced by short-range interactions.[16]

The purpose of this contribution is to examine the ability of a recently proposed coarse-grained model[12] to reproduce the phase behavior of lipid bilayers. In this coarse-grained model, which draws on the model of Smit et al.,[17] small groups of atoms (4−6 heavy atoms) are united into single interaction centers. The grouping of the atoms follows the chemistry of phosphatidylcholine lipids. All particles interact through pairwise short-range Lennard-Jones (LJ) potentials. The strength of the interaction depends on the nature of the particles. The particles differ in their degree of hydrophilicity. Hydrophilic particles are attracted more strongly to other hydrophilic particles than to hydrophobic particles.

We will study a mixture of lipids with the same headgroup but different lengths of the tails; to be specific, we use DLPC−DSPC, dilauroylphosphatidylcholine/distearoylphosphatidylcholine. As the fluid−gel transition temperature of the constituents is different, we can expect phase separation which is experimentally observed for these systems.[18−22] The experimental phase separation temperature for a 50:50 mixture is around 320 K.[18,19] At this temperature, the longer lipid freezes and leaves the shorter lipid in the fluid phase.

As we are studying lipids which are only differing in chain length, we can expect that the obtained results are qualitatively independent of the specific model and apply to all lipid mixtures with chain length differences. An increased understanding of the phase behavior of lipid mixtures will eventually lead to progress in the understanding of the self-assembled patterning of real cellular membranes.

2. Simulation Details

We performed molecular dynamics simulations using the GROMACS simulation suite[23] on mixtures of DLPC−DSPC. The initial configurations were deduced from an earlier study on pure dipalmitoylphosphatidylcholine (DPPC).[12] Model parameters are directly transferred from that work. The model was parametrized to reproduce the structural, dynamic, and elastic properties of both lamellar and nonlamellar states of a variety of phospholipids.

Figure 1 shows the coarse-grained representation of DSPC and DLPC used in this study. The PC headgroup consists of two hydrophilic groups (one for the choline group and one for the phosphate moiety). Two sites of intermediate hydrophilicity are used to represent the glycerol moiety. Each of the two tails is modeled by three (DLPC) or five (DSPC) hydrophobic sites. The solvent is modeled by individual hydrophilic sites each representing four real water molecules. The sites interact in a pairwise manner via a LJ potential. Five different LJ potentials are used, ranging from weak, mimicking hydrophobic interactions, to strong, for hydrophilic interactions, with three levels in between.

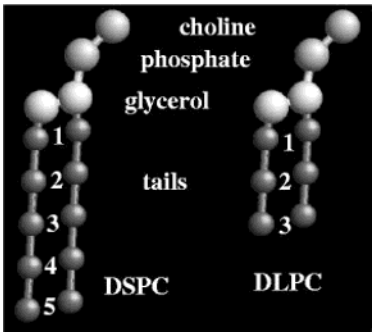

Figure 1. Illustration of the coarse-grained model and explanation of the nomenclature used in this paper. Only order parameters of interaction centers 2−4 for DSPC and interaction center 2 for DLPC are considered; only centers in the tails are used in their calculation.

In addition to the LJ interactions, a screened Coulomb interaction is used to model the electrostatic interaction between the zwitterionic headgroups. The screening of the Coulomb potential is performed by a cutoff at $r_c = 1.2$ nm. The force is smoothened to zero at the cutoff by a switching function over the whole interaction range. For this degree of modeling, we do not expect large effects of the electrostatic cutoff which were observed in atomistic simulations of bilayers.[24,25] The choline group bears a charge of +1, and the phosphate group bears a charge of −1. Soft springs between bonded pairs keep the molecules together. Angle potentials provide the appropriate stiffness. For efficiency reasons, all CG atoms have the same mass of 72 atomic units.

We are focusing on equimolar mixtures and systems with a 1:3 and 1:4 ratio of DLPC/DSPC. All concentrations in this paper are molar concentrations. For the equimolar mixture, we studied systems of different size to elucidate finite size effects. These simulations contain 64 or 256 molecules of either type. For the 1:3 ratio, one additional simulation was performed for a much bigger system containing 2048 lipids in total. All simulations include explicit solvent.

This results in system sizes of about $5 \times 6 \times 11$ nm for the smallest (128 lipids) and $13 \times 13 \times 8$ nm for the larger systems (512 lipids). The largest system (2048 lipids) measures $22 \times 23 \times 8$ nm. The similar box-lengths are in the x and y directions; the z direction is the bilayer normal. The box dimensions are coupled semi-isotropically to a pressure bath of 1 bar[26] with a compressibility of 5×10^{-6} bar^{-1}, mimicking conditions of zero surface tension. The temperature of the system is also controlled using a weak coupling scheme.[26] Coupling times were $\tau = 1$ ps for temperature and pressure, and we used a time step of 40 fs. Note that these times are not rescaled to the effective time scale below. The interaction cutoff was set to $r_c = 1.2$ nm with switching the Lennard Jones interaction smoothly to zero starting at $r_s = 0.9$ nm. We used a standard neighbor-list algorithm[27] with a cutoff $r_{NL} = 1.4$ nm.

As we derived the starting configuration from a pure system, we randomly assigned lipids to be DLPC or DSPC for most of our systems; this leads to a slight imbalance between the two leaflets of the bilayer. This imbalance persists as the flip-flop time for lipids is in the order of

(16) Reith, D.; Müller, B.; Müller-Plathe, F.; Wiegand, S. *J. Chem. Phys.* **2002**, *116*, 9100−9106.
(17) Smit, B.; Hilbers, P. A. J.; Esselink, K.; Rupert, L. A. M.; van Os, N. M.; Schlijper, A. G. *Nature* **1990**, *348*, 624−625.
(18) Mabrey, S.; Sturtevant, J. M. *Proc. Natl. Acad. Sci. U.S.A.* **1976**, *73*, 3862−2866.
(19) Ibsen, J. H.; Mouritsen, O. G. *Biochim. Biophys. Acta* (*Biomem.*) **1988**, *944*, 121−134.
(20) Bagatolli, L. A.; Gratton, E. *Biophys. J.* **2000**, *79*, 434−447.
(21) Ratto, T. V.; Longo, M. L. *Biophys. J.* **2002**, *83*, 3380−3392.
(22) Almeida, R. F. M.; Loura, L. M. S.; Fedorov, A.; Prieto, M. *Biophys. J.* **2002**, *82*, 823−834.
(23) Lindahl, E.; Hess, B.; van der Spoel, D. *J. Mol. Model* **2001**, *7*, 306−317.
(24) Anezo, C.; de Vries, A. H.; Holtje, H.; Tieleman, D. P.; Marrink, S. J. *J. Phys. Chem. B* **2003**, *107*, 9424−9433.
(25) Patra, M.; Karttunen, M.; Hyvönen, M. T.; Falck, E.; Vattulainen, I. *J. Phys. Chem. B* **2004**, *108*, 4485−4494.
(26) Berendsen, H. J. C.; Postma, J. P. M.; van Gunsteren, W. F.; DiNola, A.; Haak, J. R. *J. Chem. Phys.* **1984**, *81*, 3684−3690.
(27) Allen, M. P.; Tildesley, D. J. *Computer Simulation of Liquids*; Clarendon Press: Oxford, 1987.

Table 1. A Survey over the Simulations Presented in the Current Work

no. of DSPC	no. of DLPC	no. of water[a]	simulated temperatures [K]
64	64	1500	275, 285, 295, 305, 315, 325, 335, 345, 355, 365, 375
256	256	6000	265, 285, 305, 325, 345, 365, 385
256	64	6000	265, 285, 295, 305, 325
238	64	6000	285
384	128	3000	285, 290, 300
1536	512	12000	285

[a] Number of CG water particles. The corresponding number of real water molecules is 4 times higher.

a few hours and on our time scale no lipid hopping between the monolayers is observed. We have a 35:29 ratio in the two leaflets for the equimolar system. This means that we have concentrations of 54.6% of the "majority" component. All simulations start in the bilayer state, and we do not observe any tendency of instability of the bilayer on the time scale of the simulations which lasted for 2−4 μs.

Note that this is an effective time. The actual simulation time is 4 times less. Compared to atomistic models, the CG model is more smooth resulting in an overestimation of the dynamics. A scaling factor of approximately 4 was previously found to reproduce both lipid lateral diffusion rates and the self-diffusion of water for the CG model used in this study.[12] The times reported in this paper will therefore be effective times which are physically meaningful.

We performed simulations at various temperatures between 225 and 385 K. We were not able to equilibrate the simulations below 265 K due to the freezing of the model water, and these simulations were not investigated further. For the equimolar systems, we are presenting data for 265−385 K in which the model water is fluid. Simulations for a mixture containing 64 DLPC and 256 DSPC molecules at temperatures of 265, 285, 295, 305, and 325 K representing a 1:4 mixture with the longer lipid as the majority component are also shown. These mixtures have been produced by taking 75% of the DLPC molecules out of the equimolar simulations; the imbalance of the two leaflets leads now to the situation that we have 151 molecules in one leaflet and 169 molecules in the other. To make sure this does not affect our results, we additionally performed a simulation at 285 K with 151 molecules in either leaflet (64:238). Here the actual concentration of DLPC is 21.2%. The simulations for the 1:3 ratio have been carried out with 128 DLPC and 384 DSPC molecules. Here the concentrations in both leaflets are exactly equal. As our results do not show any irregularities, we conclude that the small imbalances are negligible for our purpose. Table 1 summarizes the simulated systems.

3. Results

As seen in Figure 2, finite size effects are found to be negligible between our equimolar simulations of 64 molecules and of 256 molecules of either type as well as for the two system sizes for the 1:3 molar ratio. For the 50:50 concentration, a phase transition between 275 and 285 K is seen by a jump in the area per headgroup. The area per headgroup is defined as the $x \times y$ box-lengths of the system divided by the number of lipids in a leaflet. Our results agree favorably with typical experimentally measured liquid- and gel-phase areas.[28] At the same time, we see a clear increase of the chain order between 265 and 285 K in the large system (below). Thus this jump indicates

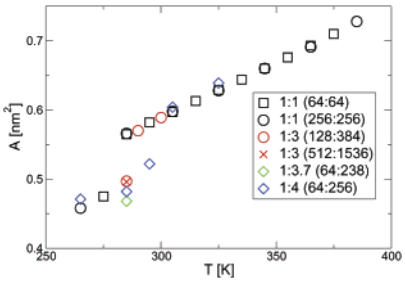

Figure 2. Area per headgroup at different temperatures and concentrations. Note that the same color stands for the same concentrations and that the types of symbols represent the different system sizes.

the transition from the fluid to the gel (or possibly crystal) phase. Experimentally, phosphatidylcholines undergo a transition to a gel phase. In simulations, it is difficult to determine clearly if the observed phase is a gel phase or possibly a full crystal. We will come to a discussion of that later. The gel phase is formed on a time scale of 500 ns to 1 μs.

Comparing the data from the 50:50 to the 20:80 mixture, we see that in the fluid phase the higher DSPC concentration takes slightly more area and that the phase transition temperature is shifted toward higher temperatures (around 295 K). The latter is clear as the longer chains have a higher propensity to form a gel phase such that a higher concentration of the long chains drives the whole system closer to the gel transition. Experimentally, the phase transition temperatures shift from about 320 to 330 K.[19]

Another experimentally very important observable is the deuterium order parameter S_{CD} which is defined as[1]

$$-S_{CD} = \frac{2}{3}S_{xx} + \frac{1}{3}S_{yy} \quad (1)$$

$$S_{\alpha\beta} = \langle 3 \cos \Theta_\alpha \cos \Theta_\beta - \delta_{\alpha\beta} \rangle \qquad \alpha,\beta = x, y, z \quad (2)$$

$$\cos \Theta_\alpha = \hat{e}_\alpha \hat{e}_z \quad (3)$$

where $\hat{e}_z$ is a unit vector in the laboratory z-direction and $\hat{e}_\alpha$ is a unit vector in the local coordinate system of the tails. It provides a measure of the alignment of the phospholipid tails in the bilayer. This quantity is accessible by NMR measurements and provides another means for quantitative comparisons between experiments and simulations. We present values for S_{CD} in Figure 3. We only calculated the order parameter for interaction centers which represent a part of the backbone and are fully surrounded by other backbone centers. For DLPC, we have only one order parameter; for DSPC we get three (cf. Figure 1). We compare the DLPC order to the DSPC order of the center closest to the head (interaction center 2), as it is well-known and also found by us that the order parameter decreases with distance from the headgroup. The order parameter closest to the headgroup shows in the liquid phase no substantial concentration dependence. Its value is around 0.2−0.3, and this agrees with typical experimental values for phospholipids.[29] The DLPC molecules have a lower degree of order in the liquid phase. The phase transition is as clearly seen in the order parameter as in the area per headgroup. The order parameter jumps at the gel transition to values of about 0.47 for DSPC; note

(28) Nagle, J. F.; Tristram-Nagle, S. *Curr. Opin. Struct. Biol.* **2002**, *10*, 474−480.
(29) Schindler, H.; Seelig, J. *Biochemistry* **1975**, *14*, 2283−2287.

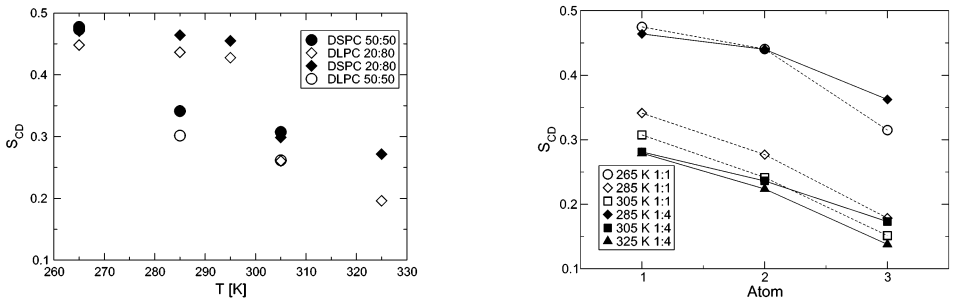

Figure 3. Deuterium order parameter. Left: Order of the first three interaction centers behind the headgroup. For 265 K, the two circles for the 50:50 system are overlapping. Right: Order of DSPC (all trimers evaluated). We average over the two tails.

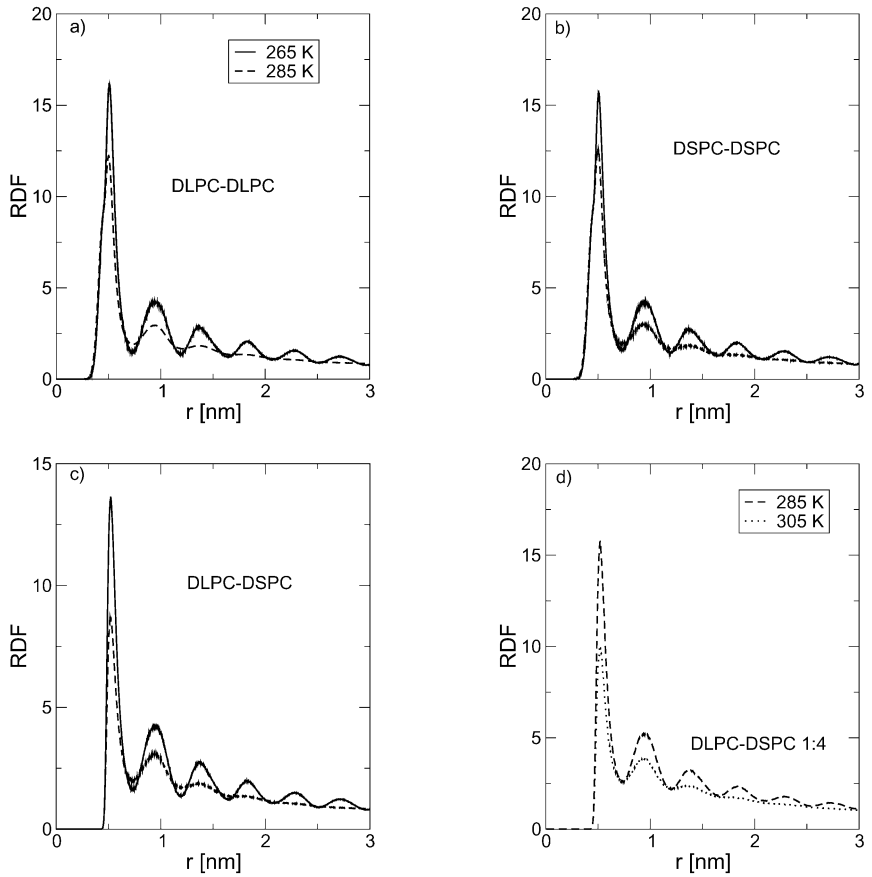

Figure 4. Radial distribution functions of the glycerol centers of the lipids for the 256:256 mixtures (a−c). (a) DLPC−DLPC, (b) DSPC−DSPC, (c) DLPC−DSPC, and (d) DLPC−DSPC for the 64:256 mixture. Running averages were used for clarity. We always chose one temperature above and one below the transition.

that $S_{CD} = 0.5$ would indicate perfect order. In the 50:50 mixture, we do not see any difference in the order of DLPC or DSPC in the gel phase (265 K); note that the symbol for DLPC is hidden under the symbol for DSPC. In the system with DSPC as the majority component, we see a slightly higher degree of order in DSPC; this suggests that liquid islands of DLPC exist in a gel-state matrix. This agrees with the slightly higher area per molecule in the uneven mixture.

Figures 4 and 5 contain atom-based radial distribution functions (rdf's); that is, we count all atom pairs falling in the respective classes. For Figure 4, the glycerol atoms are used for statistical reasons as there is the same number of them in both lipids and there is more than one per lipid. For Figure 5, the phosphates are used to prevent intramolecular effects. The data show that the lipids are close to ideally mixed at any temperature in the equimolar system. They always very slightly prefer surroundings of the same type. At 265 K, in the higher ordered phase we see a longer range ordering again confirming that we encounter a structural phase transition. At 285 K in the 1:4 mixture (Figure 5b), we see a slight preferential surrounding of lipids in a 2 nm neighborhood with like lipids as a possible indication of phase separation.

Generally we find that the distance between neighboring lipids is around 0.52 nm and in the liquid case there is a second peak at 0.97 nm. Higher order peaks are only weakly visible. In the low-temperature structure, we see a set of peaks. The dynamics (below) indicates that we actually do not freeze completely to a crystalline structure.

So in the equimolar mixture, we find that the phase transition we see is actually a gel (or crystal) to liquid crystalline transition and the two constituents freeze together. Figure 6 shows the difference of the gel (or crystalline) and liquid phases in the equimolar mixture just above and below the phase transition. At the lower temperature, a local hexagonal structure is seen. We are not able to see real phase separation in this system;

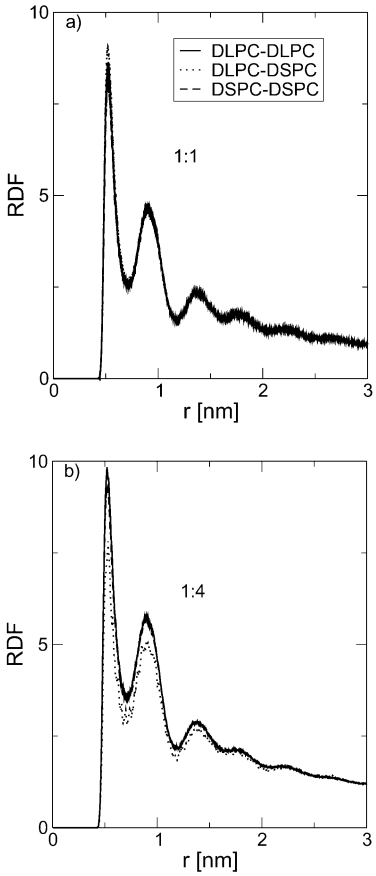

Figure 5. Radial distribution functions of the phosphate centers of the lipids below the transition: (a) 256:256 system at 265 K and (b) 64:256 system at 285 K.

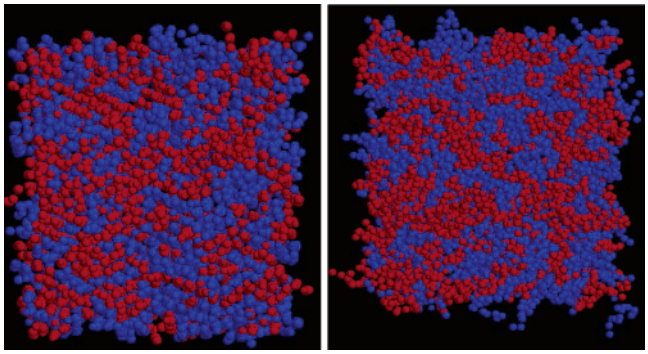

Figure 6. Snapshots of the 50:50 mixtures at 265 K (left) and 285 K (right). Water has been removed for clarity; DLPC is seen in red and DSPC in blue.

however the nonideal mixing of the two components is visible, both below and above the phase transition.

For the 1:4 mixture, we find also in the rdf the signature of the higher phase transition temperature (cf. Figure 4d). It is between 295 and 305 K, consistent with the order parameter and the area per headgroup data. At 285 K, we see some hints that we have a mainly gel-phase system with a few islands of liquid DLPC remaining. We see the same at 285 K in the 1:3 mixture. For a large-scale phase separation, the systems are too small. We expect that limitations in simulation length and system size prevent us from seeing the phase separation in the equimolar system. Figure 7 shows on the left-hand side a simulation at the 1:3 concentration where we actually can identify a liquid domain in a gel matrix. Here for clarity only the C_2 carbons of one leaflet are shown. The liquid domain is

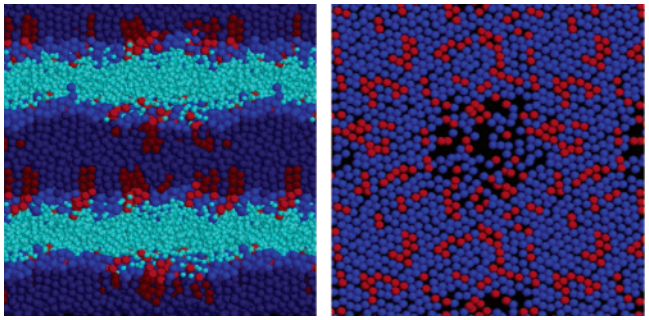

Figure 7. Snapshots of the 1:3 (DLPC/DSPC) mixture: DSPC, blue; DLPC, red; water, light blue. Left: Side view of a simulation. Right: Top view showing lateral ordering; only the C_2 atoms are shown of one of the two leaflets, clearly showing the hexagonally ordered gel phase surrounding a disordered fluid region. The concentration of DLPC in this region is approximately 1:2 (DLPC/DSPC).

less ordered and has a lower density. The side view (cf. Figure 7, left) shows a tendency for registration of the patches with higher DLPC or DSPC concentration between different leaflets. The local concentration of DLPC in the fluid domain is increased and estimated to be about 1:2 (DSPC/DLPC), a 50% increase.

The domain separation observed in the 1:3 system at $T = 285$ K is found to be independent of the system size. The 4 times bigger system also develops a big gel domain surrounding a small DLPC-enriched fluid region. The size of the fluid domain is similar in the big system compared to the smaller one. The size of the gel-phase cluster scales with the system size as is typical of a system in which the dominant phase fraction is above the percolation threshold.[8]

The density profiles across the bilayer (cf. Figure 8) show that with decreasing temperature we find an increasing concentration of DSPC in the middle. As we see at the same time that the headgroups of both lipids are at the same distance from the middle (cf. Figure 9), this suggests that the stretching DSPC molecules increase the bilayer thickness to a point where DLPC eventually cannot reach to the middle anymore. This point is concomitant with the freezing transition of the bilayer for the equimolar mixture. Additionally we see at that temperature a qualitative change in the transversal structure of the bilayer. This has been observed in atomistic simulations of pure DPPC before.[30] Figure 9 shows that at the phase transition the bilayer becomes thicker. It rises from 4.37 nm at 285 K to 5.04 nm at 265 K. We define the bilayer thickness as the distance between the planes of the phosphorus centers. Additionally we see that the planes of the phosphorus and the nitrogens become more well-defined, and the freedom perpendicular to the bilayer shrinks.

To characterize the phase behavior and the actual phases in more detail, we elucidated the diffusion and rotation behavior of the various molecules. Figure 10 shows the mean square displacement of the DSPC and DLPC molecules at various temperatures for the large equimolar system. Keeping in mind that the dimensions of these systems are about 12 nm, we see in the fluid phase that the molecules diffuse completely around our system. At low temperature, we observe that they are at least moving around 3 nm in the plane, suggesting that we do not have a crystalline phase although some hexagonal ordering is

(30) Sum, A. K.; Faller, R.; de Pablo, J. J. *Biophys. J.* **2003**, *85*, 2830−2844.

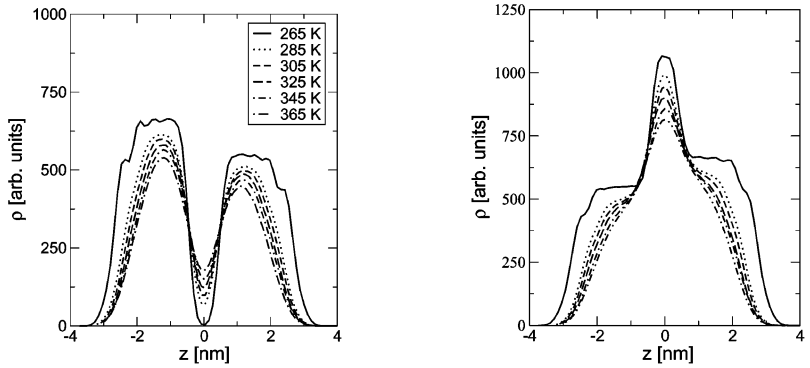

Figure 8. Density profile for DLPC (left) and DSPC (right) in the 256:256 mixtures. The plane of lowest density of DLPC is set to zero; the asymmetry stems from the random assignment of DLPC and DSPC to the leaflets (see the text). The legend applies to both graphs. Note that as all interaction centers have the same mass in the simulation, density profiles are in arbitrary units.

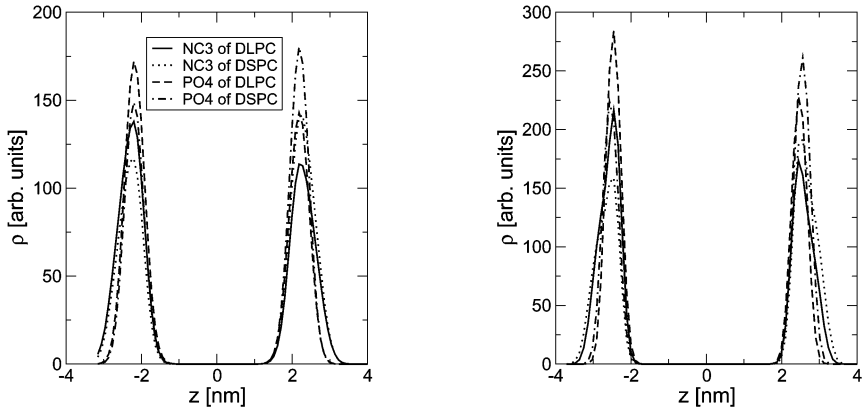

Figure 9. Density profile of the headgroups at 285 K (left) and 265 K (right). Note the difference in scale on the *y*-axis. The units are arbitrary but the same for both graphs.

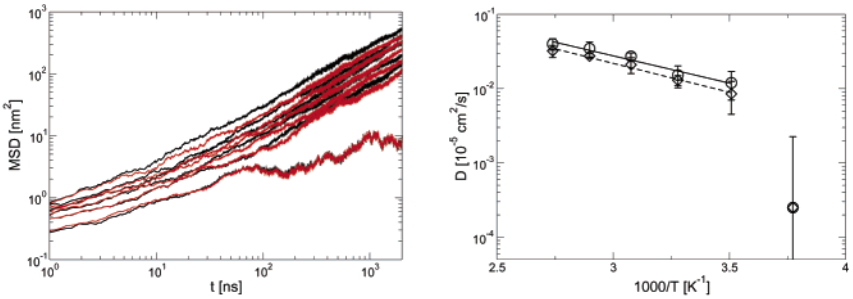

Figure 10. Left: Mean square displacement of the lipids for the 256:256 mixtures. DLPC, black; DSPC, red. The temperature rises from bottom to top in 20 K steps between 265 and 365 K. Right: Arrhenius plot of the corresponding diffusion coefficients fitted between 400 and 2000 ns. The lines are fits disregarding the lowest (gel-phase) temperature.

observed. It is more probably a hexatic liquid crystal phase. The diffusion behavior of DLPC and DSPC is quite similar in both phases. In the liquid phase, the diffusion obeys an Arrhenius behavior confirming a true two-dimensional liquid phase.

The reorientation correlation function of the first Legendre polynomial

$$C_1(t) = \langle \vec{u}(t)\vec{u}(0)\rangle \tag{4}$$

(cf. Figure 11) makes it clear that the headgroup dynamics and the tail dynamics decouple at the phase transition. For all temperatures, the decay of the P−N vector goes to the same residual value ($C_1 \approx 0.07$) in a short time (<10 ns). The residual value indicates the overall average orientation of the headgroup vector. To see a decay to zero flip-flops would be necessary. Still, we see a clear difference in the dynamics of the gel and the liquid crystal phase. The lowest temperature (265 K) is distinctly slower than the temperatures in the liquid phase, but full reorientation is attained. We do not see differences between DLPC and DSPC for the headgroups (not shown).

The in-plane reorientation of the whole lipids is monitored by the vector connecting the C_1 centers on both tails. For the high-temperature phase, that is, the liquid phase, in the 50:50 and the 20:80 mixture, we see a very fast decay on a time scale comparable to the headgroup reorientation. The very low residual indicates that the C_1-C_1 vector is preferably parallel to the bilayer plane. For clarity, we do not distinguish between lipid types here. For the 50:50 mixture at 265 K, there is again little distinction between lipid types; however, DSPC is slightly slower. Full reorientation cannot be attained on reasonable time scales; we have to extrapolate a reorientation time on the order of a few microseconds.

We find a very interesting behavior for the 1:4 mixtures at 295 K. First we see a clear signature of dynamic

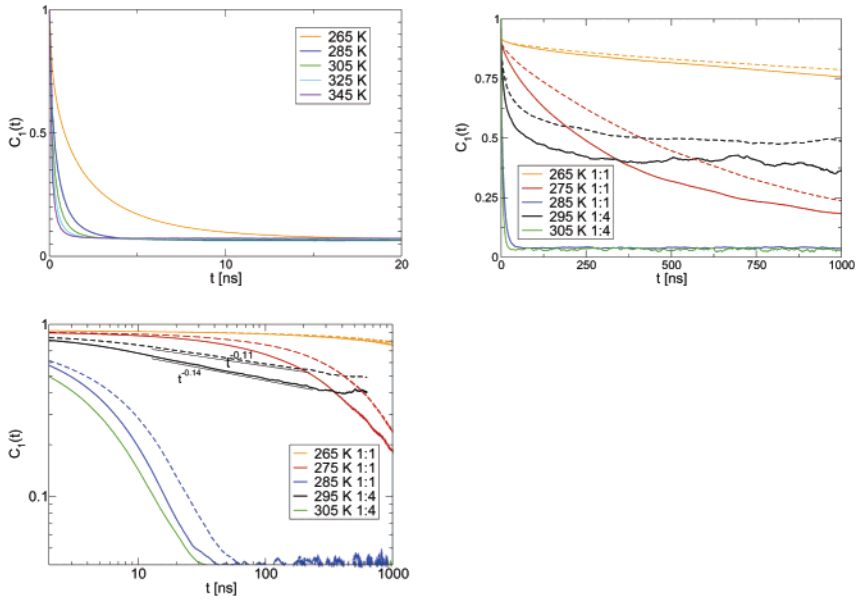

Figure 11. Reorientation correlation function at various temperatures in the 256:256 and 64:256 mixtures. Upper left: The P−N vector in the headgroup. Upper right: The vector connecting the two C_1 centers in the tail. In the cases where there are two lines in the same color, the slower reorientation (dashed line) is DSPC. Otherwise the difference is indistinguishable on this scale and we use the average. Lower: Double logarithmic representation of the C_1-C_1 reorientation functions. Note that the 275 K 1:1 system has only 64 lipids of either type. Algebraic fits (thin lines) are shown to the intermediate region at $T = 295$ K; they are shifted slightly for clarity.

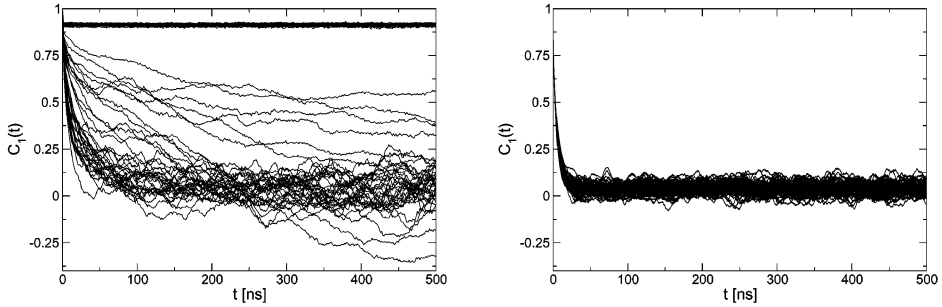

Figure 12. Individual reorientation correlation functions for the vectors connecting the C_1 atoms in the DLPC molecules. Left: 295 K, 20% DLPC. Right: 305 K, 50% DLPC.

heterogeneity between the two types of lipids (Figure 11). DSPC is significantly slower in its reorientation which again hints at domain formation. We cannot calculate the reorientation time as we do not reach full reorientation; however, we see (Figure 11, lower figure) that the reorientation at 295 K at intermediate time scales (10−200 ns) exhibits an algebraic decay $C_1 \propto t^{-\alpha}$ with slightly but distinguishably different exponents: $\alpha_{DLPC} = 0.14$ and $\alpha_{DSPC} = 0.11$. This again suggests that the dynamics of DLPC and DSPC decouple. At very long times ($T > 500$ ns), we see indication of a plateau which hints toward an intermediate range of no reorientation at all. We do not see this kind of algebraic decay for 1:1 mixtures in either phase.

Moreover, we see dynamic heterogeneity within the same type of lipid. Studying the variety of individual reorientation functions, that is, all individual C_1-C_1 vectors, we find that the DLPC reorientation functions at 295 K are falling into two different categories, one with almost no reorientation of the tails and one with relatively fast reorientation. This clearly shows us the formation of patches as at 305 K we do not find a dynamic heterogeneity in the set of DLPC alone (cf. Figure 12). A more thorough investigation of the influence of the respective neighborhoods as has been done recently for polymers[31] is currently underway.[32]

Whether or not the apparent liquid−gel phase coexistence observed in some of our simulations is of truly thermodynamic origin requires further study. Preliminary data on freezing of large patches of single-component bilayers for instance indicates that small regions of fluid lipids remain trapped inside a gel matrix as soon as the gel phase percolates the system in two dimensions. Monte Carlo techniques may be required to obtain the thermodynamic equilibrium state of these systems. Larger simulations and more concentrations and temperatures are needed in order to map out the entire phase diagram. This endeavor is being undertaken.

4. Conclusions

We have shown the ability of a recently proposed lipid bilayer model to reproduce semiquantitatively the phase behavior of mixtures of phosphatidylcholines of different chain lengths. The phase transition from the liquid crystalline to the gel phase shifts to lower temperature with increasing concentration of short-chain lipids. Lipids

(31) Faller, R. *Macromolecules* **2004**, *37*, 1095−1101.
(32) Faller, R. Manuscript in preparation.

of different chain lengths mix almost perfectly in the liquid phase. At the transition region, we can for systems with a majority of longer lipids identify islands of disordered lipids in a gel-phase matrix; we are not yet able to see this phase separation for equimolar systems, and we suspect that this stems from computational limitations. For the demixing systems, we find consistent a dynamic heterogeneity of fast and slow lipids. The transition influences the dynamics of the chain tails, but the reorientation dynamics of the headgroups is not influenced by the phase behavior. At the gel temperatures, we find that the stretching of the longer chains leads to an additional demixing perpendicular to the bilayer plane as the shorter chains cannot reach the center any more.

LA0492759